

# Human-earth system feedbacks in HDD/CDD

Corinne Hartin<sup>1,2</sup>, Robert Link<sup>1</sup>, Pralit Patel<sup>1</sup>, and Russell Horowitz<sup>1</sup>

<sup>1</sup>Pacific Northwest National Laboratory

<sup>2</sup>Corresponding author

January 12, 2018

# 1 Introduction

The human and earth systems are intricately linked, where human decisions influence the earth and changes in the earth influence human decisions. The building sector is particularly susceptible to human-earth system feedbacks due to the fact that the demand for cooling and heating is directly related to temperature. With increasing temperatures, the global demand for heating is projected to decrease, while the demand for cooling is projected to increase (Li, Yang, & Lam, 2012; Isaac & van Vuuren, 2009). The building sector is not insignificant, for example in the USA, heating and cooling energy accounts for about 49% of all final energy in residential buildings and 44% in commercial buildings in 2005 (Kyle et al., 2010). these increased temperatures will alter the balance between heating and cooling needs, causing regions with moderate climates to warm, shifting some locations from primarily heating to primarily cooling (Auffhammer & Mansur, 2014).

Typically research in building impacts has been conducted in one way, where changes in income and population influence the building sector. For example, (Yu, Eom, Zhou, Evans, & Clarke, 2014) investigated different building energy scenarios across China. (Sharma, Chaturvedi, & Purohit, 2017) investigated changes in CO<sub>2</sub> and HFC emissions under different economic assumptions in India. Or studies have looked at the system in the opposite direction, trying to understand the effects of a temperature change on the building sector. For example, (Petri & Caldeira, 2015) used CMIP5 model output under RCP8.5 to investigate how HDD and CDD will vary regionally across the US. However, within in all of studies heating and cooling degree days are exogenous to the model so therefore feedbacks between changes in temperature and heating and cooling degree days are not represented.

These approaches fail to link the important two-way coupling between the human and earth systems at every modeling time step. Recently, studies have identified the need for these fully coupled, interacting systems (Palmer and Smith 2014; Hallegatte and Mach 2016; add in the snowmass report). In the study by (Labriet et al., 2013), they investigated the feedbacks between heating and cooling demands and CO<sub>2</sub> emissions, and found close to no change in global CO<sub>2</sub> emissions. However, they only investigated the feedbacks with regards to CO<sub>2</sub> and did not include feedbacks from emissions produced directly from increased cooling services. For example, hydrofluorocarbons (HFCs) are used as coolants across the world in refrigeration, cooling units,

and heat pumps, and are released during the operational lifetime of the equipment, during servicing or at the end of the equipment’s life. HFCs typically have much longer lifetimes and stronger radiative forcing properties than CO<sub>2</sub>, making them an extremely effective greenhouse gas.

Our approach relies on a fully coupled human-earth system in which we explore the two-way feedbacks between the building sector and the earth system within GCAM (Edmonds et al., 2004). We implemented a coupled modeling framework with statistical relationship between global mean temperature change and heating and cooling degree days at every time step, allowing us to investigate impacts from this feedback on both the human and earth systems.

## 2 Methodology and Data

### 2.1 Modeling Framework – GCAM and Hector

Assessing the combined impacts of socioeconomic changes, technological changes, earth system changes, and other factors on the global buildings sector requires an internally consistent framework that can account for these factors simultaneously. The global building energy model used in this study has been constructed within the Global Change Assessment Model (GCAM) (Calvin et al., 2016). GCAM is a dynamic-recursive market equilibrium model, combining models of the global energy system (J. and J., 1985; Edmonds et al., 2004), global land use (M.A. Wise, 2011), and a reduced-form representation of the earth system (Hartin, Patel, Schwarber, Link, & Bond-Lamberty, 2015). GCAM represents supplies and demands for energy in each of 32 geopolitical regions. Demands are linked to region-specific assumptions of population growth, labor participation rates, and labor productivity growth. Other important inputs include technology cost and performance information, fossil and other resource information, and climate or other policies. The model is solved by finding a set of prices in all markets at which supplies match demands. GCAM is run in five-year time steps from 2010 to 2100. A detailed description and model code can be found at <http://www.globalchange.umd.edu/models/gcam>.

### 2.2 Modeling global building energy consumption

This study builds on the technologically-detailed, service-based building energy modeling approach implemented previously for China, India, and the U.S. in GCAM (Eom, Clarke, Kim, Kyle, & Patel, 2012;

Chaturvedi, Eom, Clarke, & Shukla, 2013; Zhou, Eom, & Clarke, 2013), simplifying its detail and applying it to all regions (Figure 1). Underlying socioeconomic drivers – population and income – drive the demand for floorspace in representative residential and commercial buildings in each of GCAM’s 32 regions. There are three types of energy service demands associated with this floorspace: space heating, space cooling, and “other” services, which includes services such as appliances, lighting, and water heating. The change in demand for these per unit of floorspace is related to the change in affordability of the energy services (the ratio of per capita income to the price of providing the service) and to heating and cooling degree days. The latter dependence allows the model to represent the impact of temperature change on service demands (Eom, Clarke, Kim, Kyle, & Patel, 2012), and hence on energy expenditures.

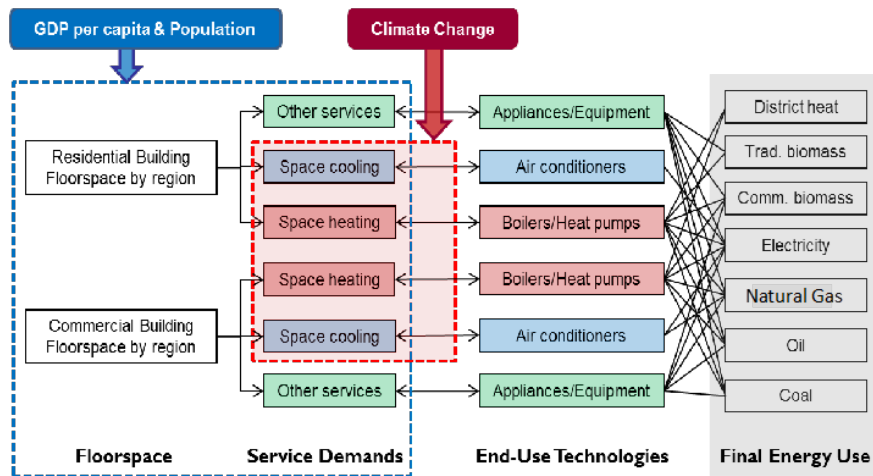


Figure 1: Structure of the energy supply and demand within the building energy model within GCAM. Figure from Clarke et al., 2017. - not published yet. We should probably change the red box.

### 2.3 2.3 GCAM Fusion - PRALIT - do we want a description of this in the paper?

### 2.4 Degree Days

Degree days are a metric that indicates requirements for building heating or cooling. Annual degree days are the summation of temperature difference from a balance point over time and capture both the extremity and duration of difference between outdoor temperatures and a reference temperature (Baumert and Selman 2003; Say 2006). In order to couple GCAM and Hector, this study required a relationship between global mean temperature (a Hector output) and degree days (a GCAM input). This led to the development of a

GLM (generalized linear model) to model both HDDs and CDDs for various ESMs used in CMIP5 (Table 1). In order to obtain annual HDDs/CDDs for each GCAM region, daily average temperature data from the ESMs was regridded to a  $0.5^\circ \times 0.5^\circ$  grid and used to calculate HDD/CDD within each grid cell using the formula below, with balance temperature,  $T_b$  ( $18.3^\circ \text{ F}$  or  $65^\circ \text{ F}$ ) and surface temperature,  $T_s$ :

$$HDD = \begin{cases} T_b - T_s & \text{amp; if } T_s < T_b, \\ 0 & \text{amp; if } T_s \geq T_b \end{cases}, \quad CDD = \begin{cases} T_s - T_b & \text{amp; if } T_s > T_b, \\ 0 & \text{amp; if } T_s \leq T_b \end{cases}, \quad (1)$$

The HDDs/CDDs in each grid cell were then summed annually and population-weighted from grid cell to GCAM region in each year. Annual global mean temperature was also calculated for each ESM.

We treated the HDDs and CDDs as count data. For each region, there is a count, which is never less than zero, of HDDs and CDDs for each year. As a result, a Poisson regression model was chosen for the GLM, with a logarithmic link function and random error possessing a Poisson distribution. Let  $N_H$  and  $N_C$  be the numbers of heating and cooling degree days in region  $r$ , with population-weighted latitude  $L_r$ . Then:

$$\ln(N_H) = \alpha_1 T + \alpha_2 T L_r + \alpha_3^{(r)} T^2 + \alpha_4^{(r)}, \quad (2)$$

and

$$\ln(N_C) = \beta_1 T + \beta_2 T L_r + \beta_3^{(r)} T^2 + \beta_4^{(r)}, \quad (3)$$

where  $T$  is the global mean temperature. The  $\alpha$  and  $\beta$  are regression coefficients. Coefficients with a  $(r)$  superscript are region-specific, while those without are the same for all regions.

At every time step, global emissions are used to calculate the global mean temperature from Hector, from which heating and cooling degree days in each of the 32 regions are calculated within GCAM. The energy system responds to this change in heating and cooling demands in each region.

## 2.5 Scenarios

Due to the coupled nature of the system, we can run numerous scenarios and investigate the uncertainty associated with choice of climate model (Table 1), equilibrium climate sensitivity, and socioeconomics. For each scenario, climate sensitivity was set to the range of climate sensitivity values for the CMIP5 models (Table 9.5-1, IPCC) of  $2.1$  and  $4.7^\circ \text{ C}$  plus the default Hector value of  $3.0^\circ \text{ C}$ . Population and GDP follow the assumptions of the Shared Socioeconomic Pathways (SSP) 1, 2 and 5 (Riahi et al., 2017). At a global level for SSP1, population is assumed to peak in 2050 and decline to about 7 billion people by the end of

Model	Modeling Center
ACCESS 1-0	Australian Community Climate and Earth System Simulator Coupled Model, Australia
CanESM2	Canadian Centre for Climate Modeling and Analysis, Canada
CCSM4	NSF/DOE, National Center for Atmospheric Research, USA
CESM1- CAM5	NSF/DOE, National Center for Atmospheric Research, USA
CMCC- CMS	Centro Euro-Mediterraneo sui Cambiamenti Climatici Climate Model, Italy
CNRM- CM5	Centre National de Recherches Météorologiques, France
GFDL- CM3	NOAA, Geophysical Fluid Dynamic Laboratory, USA
HadGEM2- ES	Meteorological Office Hadley Centre, U.K.
inmcm4	Institute of Numerical Mathematics, Russia
IPSL- CM5A- MR	Laboratoire de Meteorologie Dynamique, Institut Pierre-Simon Laplace, France
MIROC- ESM	Atmosphere and Ocean Research Institute, National Institute for Environmental Studies and Japan Agency for Marine-Earth Science and Technology, Japan
MPI- ESM-MR	Max Planck Institute for Meteorology, Germany
NorESM1- M	Norwegian Climate Centre, Norway

Table 1: Table of CMIP5 models emulated in this analysis.

the century ([van Vuuren et al., 2017](#)). This reference scenario run in GCAM results in a radiative forcing change of  $6.43 \text{ W m}^{-2}$  and a  $3.86 \text{ }^\circ\text{C}$  temperature change in 2100. At a global level for SSP2, population is assumed to peak in 2070 and then decline to about 9 billion people by the end of the century, with the growth occurring mostly in a subset of the developing regions ([Fricko et al., 2017](#)). This reference scenario run in GCAM results in a radiative forcing change of  $6.31 \text{ W m}^{-2}$  and a  $3.68 \text{ }^\circ\text{C}$  temperature change in 2100. At the global level for SSP5, population is assumed to peak in about 2050 and decline to 7.4 billion people by the end of the century. SSP5 is characterized by high levels of fossil fuel use and greenhouse gas emissions over the century ([Kriegler et al., 2017](#)). This reference scenario run in GCAM results in a radiative forcing change of  $7.35 \text{ W m}^{-2}$  and a  $4.37 \text{ }^\circ\text{C}$  temperature change in 2100. Since we aren't changing energy-related assumptions, the SSP1 used here has a higher radiative forcing than the official SSP1 and the SSP5 has a lower radiative forcing than the official.

For the feedback scenarios, we turn on the relationship between global mean temperature change and heating and cooling degree days, allowing the model to endogenously calculate these within each region for each

climate sensitivity and SSP combination. Both reference and feedback scenario are run emulating each of the 13 CMIP5 models. All figures and discussion are comparing the reference case from the feedback case.

### 3 Results

#### 3.1 Global impacts

We start with highlighting the one scenario, SSP2 and a climate sensitivity of  $3.0\text{ }^{\circ}\text{C}$  across all climate models. As global mean temperature rises, the demand for heating in the high latitude regions decreases while the demand for cooling in the mid latitudes increases (not shown atm). This change in heating and cooling demand is further amplified by incorporating feedbacks between global mean temperature change and heating and cooling degree days, leading to an increase in the median global temperature of  $0.063\text{ }^{\circ}\text{C}$  in 2100 with a range of  $0.052\text{ }^{\circ}\text{C}$  and  $0.079\text{ }^{\circ}\text{C}$  (Figure 2).

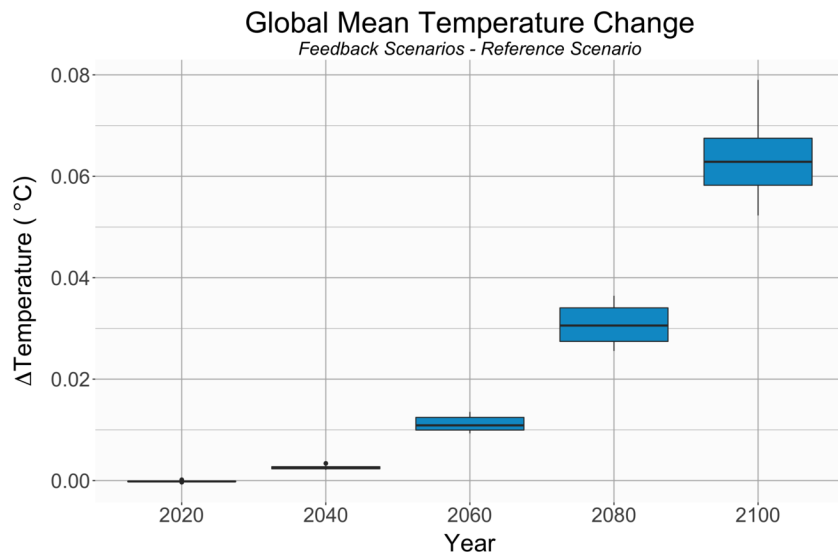


Figure 2: Building energy feedback effects on global mean temperature ( $^{\circ}\text{C}$ ) for scenarios with SSP2 and climate sensitivity  $3\text{ }^{\circ}\text{C}$ .

This modest change in global mean temperature leads to significant changes in the energy system. Figure 3 shows the increase in cooling demands by a median of 6.9 EJ, while the demand for heating decreases by a median of 10.3 EJ. This shift in heating and cooling energy use has important implications for fuel mix

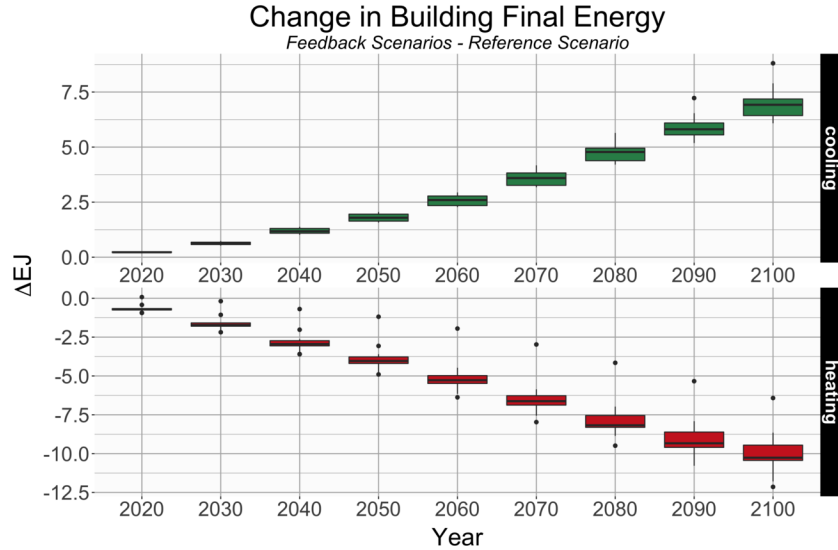


Figure 3: Building energy feedback effects on global total energy (EJ) to building a) cooling and b) heating for scenarios with SSP2 and climate sensitivity  $3^{\circ}\text{C}$ .

(Figure 4). If we break apart the global energy demand into their various components, we see the proportions of energy use shift to higher demands in electricity, while all other energy inputs decrease. Final energy to the building sector is roughly balanced out by the increased demands for cooling and the decreased demands for heating. Similar to (Labriet et al., 2013), we find no significant change in global  $\text{CO}_2$  emissions (Figure 6).

However, there are some emissions that are linked directly to increases in cooling demands. The cooling service is almost entirely delivered by electricity, whereas heating service is delivered by other primary and secondary fuels, such as gas, coal and biomass. This increase for cooling demand leads to a median increase in 2100 HFC134a and 143a emissions of 863 and 181 Gg (Figure 5). The increase in global mean temperature is due to the change in HFC emissions and not due a change in  $\text{CO}_2$  emissions.

### 3.2 Uncertainty quantification

Due to the fact that these models are coupled in code we can easily run numerous scenarios we can run numerous scenarios. If we consider all 126 scenarios, the difference in global mean temperature change in 2100 between the feedback and reference cases, ranges from  $0.023^{\circ}\text{C}$  to  $0.302^{\circ}\text{C}$ . We can break down the relative importance of the sources of uncertainty across all 126 scenarios with a classic anova analysis (Figure 7). We see that a change in climate sensitivity leads to the largest variance, with greater than

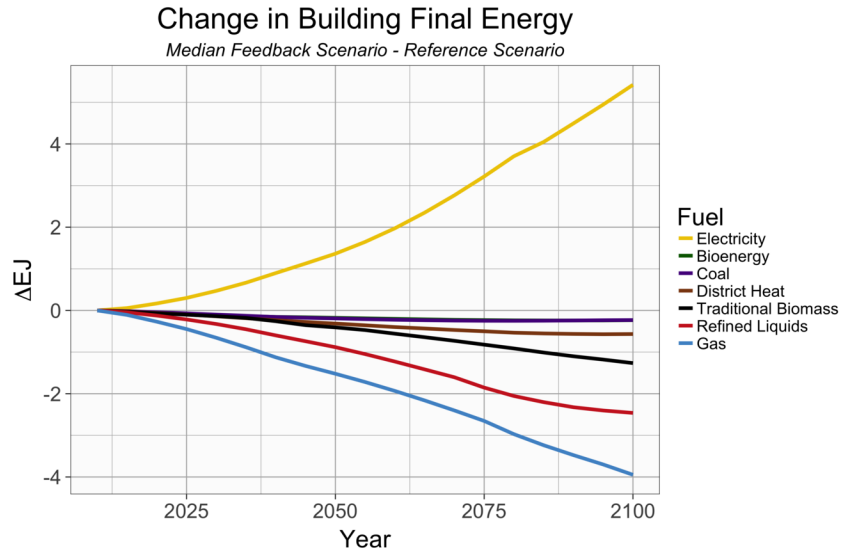


Figure 4: Building energy feedback effects on global building energy demand (EJ) for scenarios with SSP2 and climate sensitivity  $3^\circ\text{C}$ .

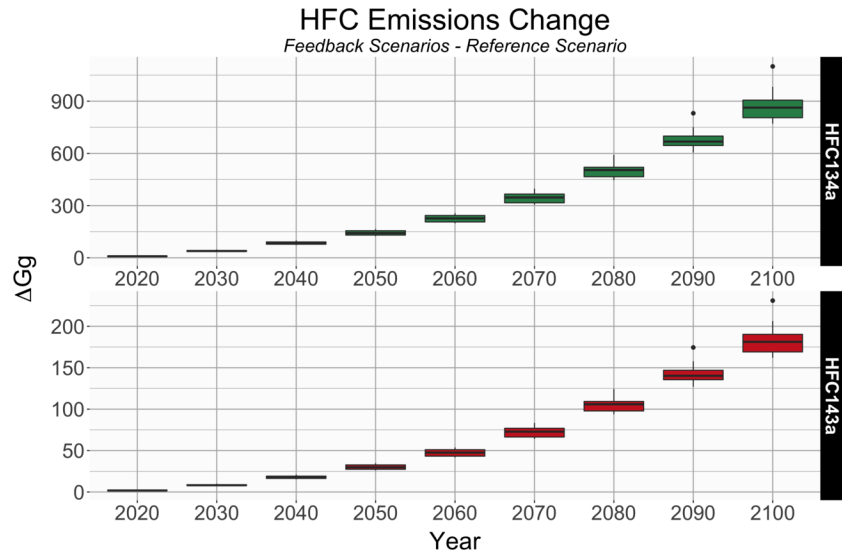


Figure 5: Building energy feedback effects on a) HFC134a emissions (Gg) and b) HFC143a emissions (Gg) for scenarios with SSP2 and climate sensitivity  $3^\circ\text{C}$ .

0.45K<sup>2</sup> in 2100.

We can investigate sources of uncertainty across all GCAM outputs. For example, we can investigate the the breakdown in variance for cooling and heating energy demands (Figure 8). Like global mean temperature change, variance in cooling and heating energy demands is dominated by uncertainty in climate sensitivity,

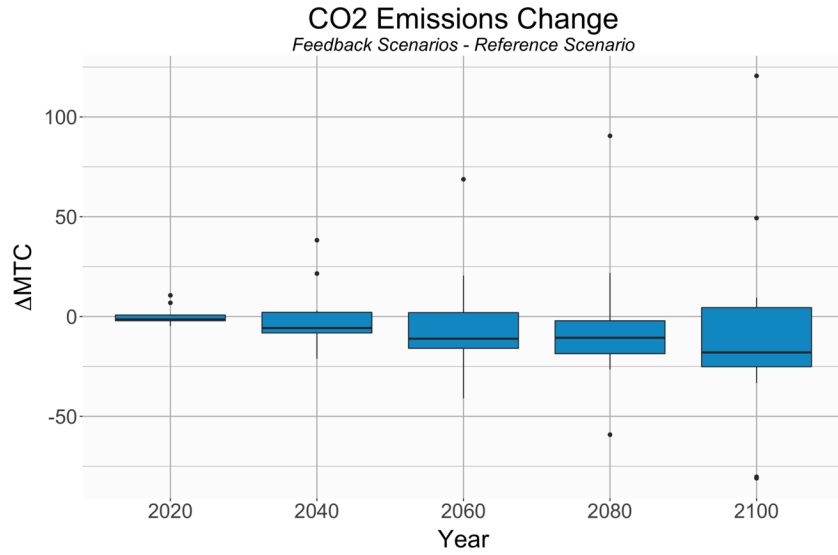


Figure 6: Building energy feedback effects on global CO<sub>2</sub> emissions (MtC) for scenarios with SSP2 and climate sensitivity 3 ° C . 3 ° C .

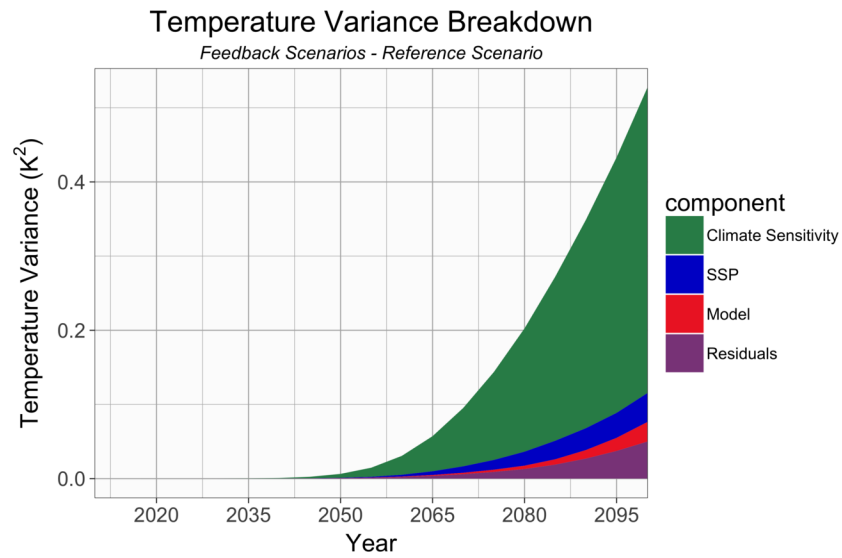


Figure 7: Total variance for global mean temperature change split into 4 sources of uncertainty, climate sensitivity, SSPs, model, and anova residuals.

however, we see differences between heating and cooling. WHAT ELSE DO I WANT TO SAY?

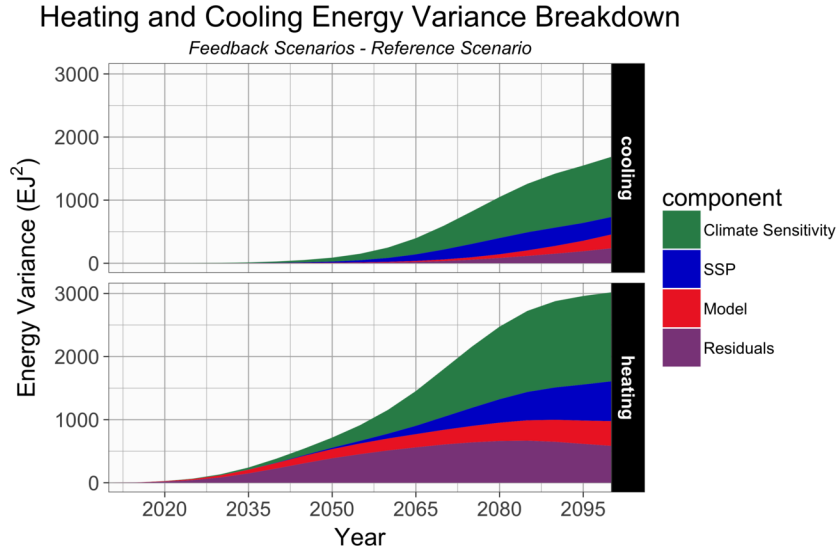


Figure 8: Total variance for a) cooling and b) heating energy demands split into 4 sources of uncertainty, climate sensitivity, SSPs, model, and anova residuals.

### 3.3 Regional impacts

GCAM's energy and economic sector is broken up into 32 regions, in which we can investigate regional with the system. We see in Figure 6 that CO<sub>2</sub> emissions globally are close to zero. However, if we look regionally we can see differences under an SSP2 and climate sensitivity of 3.0C. Africa, India and Indonesia have an increase in CO<sub>2</sub> emissions while the USA, Canada, Europe, Asia and Russia all see a decrease in emissions. An increase in HFC134a emissions corresponds to the regions with an increase in electricity demands for cooling. Western Africa and India see both the largest increase in electricity demands for cooling, at 1.15 EJ and 0.67 EJ respectively, as well as the largest increase in HFC134a emissions, at 165 Gg and 100 Gg respectively.

## 4 Discussion and Conclusions

The GCAM modeling framework allow us the opportunity to investigate human-earth system feedbacks. To highlight this capability we explore the effects of building energy feedbacks on the human-earth system. When accounting for the feedbacks between increased cooling demands and HFC emissions, global mean temperature increases across all scenarios. The increase in temperature leads to increased cooling demands for electricity while heating demands for delivered gas and coal decrease.

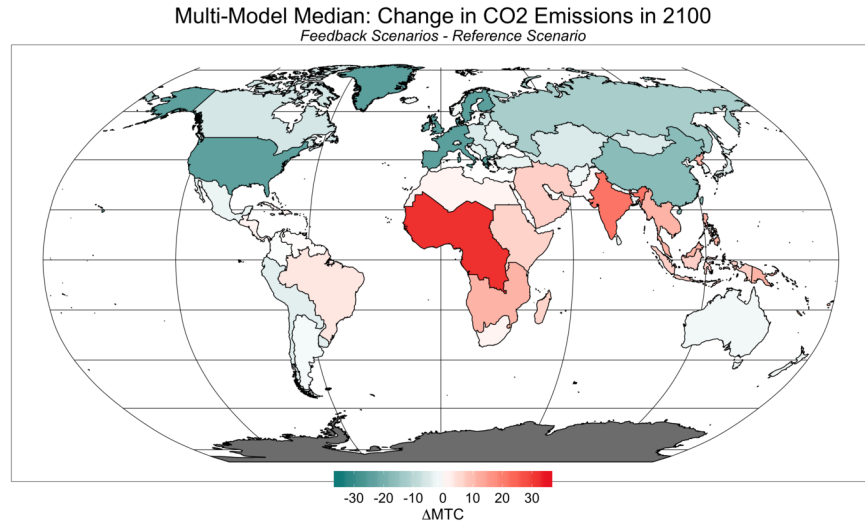


Figure 9: Multi-model median difference between the feedback scenario and the reference for CO<sub>2</sub> emissions (MtC) in 2100.

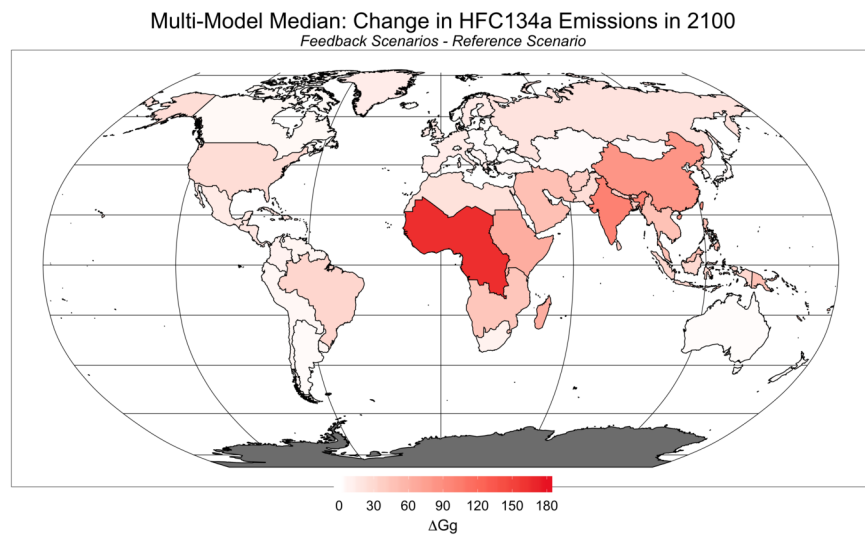


Figure 10: Multi-model median difference between the feedback scenario and the reference for HFC134a emissions (Gg) in 2100.

In this study we investigated 3 sources of uncertainty, 1. choice of ESM emulated, 2. choice of climate sensitivity, and 3. socioeconomic assumptions . The different ESMs emulated provide different results for the same emission pathway. Heating and cooling degree days along with energy demands are influenced by model choice. This has also been documented in (Zhou, Eom, & Clarke, 2013), however, in a one way

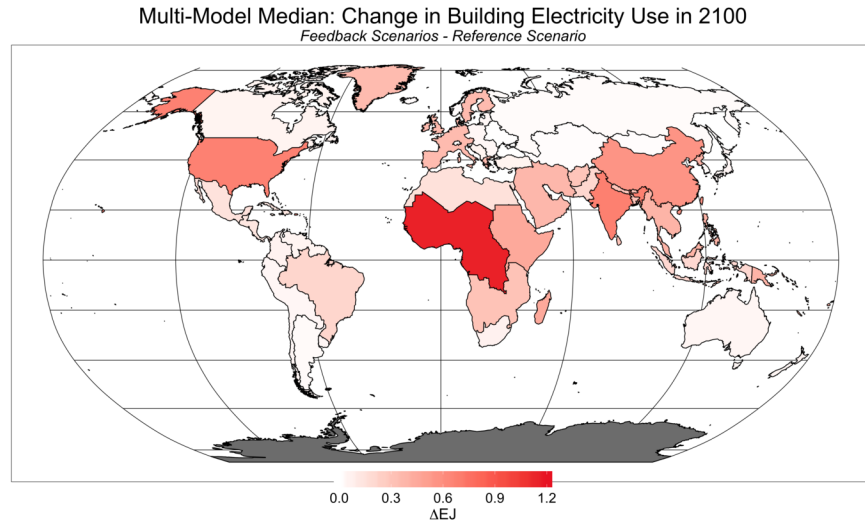


Figure 11: Multi-model median difference between the feedback scenario and the reference for electricity demand (EJ) for building cooling in 2100.

coupled simulation. The choice of climate sensitivity provides us with information on how the earth system will respond to under the same emission pathway. Lastly, the choice of socioeconomics will influence both the calculation of heating and cooling degree days in each region across difference emission pathways.

Most building energy studies emphasize the need for a regional focus when investigating energy demands under a changing climate. (Isaac & van Vuuren, 2009) assessed global energy consumption for residential heating and air conditioning under a changing climate and found considerable impacts in energy demands on regional scales. (*Industry, settlement and society. Climate Change 2007: Impacts, Adaptation and Vulnerability . Contribution of Working Group II to the Fourth Assessment Report of the Intergovernmental Panel on Climate Change, 2007*) emphasized the need to consider different fuels to use for heating and cooling, since an increase in cooling demand may lead to an increase in electricity demand. (Zhou, Eom, & Clarke, 2013) explored the effects of various climate scenarios on building energy demands in China and the U.S. within the GCAM integrated assessment model, finding a 6% decrease in the building sector’s final energy consumption. (Olonscheck, Holsten, & Kropp, 2011) analyzed the combined effect of future changes of climate, building stock, renovation measures, and heating energy systems on residential energy demand in Germany based on a simple building energy system model. In this study we find that Africa and India have increased electricity demands and increased emissions when accounting for this simple feedback. Previous studies investigating impacts may underestimate the energy demands under a changing climate.

There are some limitations of an aggregate study. This study focuses on gross energy consumption and not on the temporal or spatial characteristics of heating and cooling load. For example, heat waves would increase peak load, resulting in different technology investment profiles and emissions (Zhou, Eom, & Clarke, 2013). Future efforts to reduce HFCs such as the Kigali amendment to the Montreal protocol would have implications on our results, but are not considered in the current analysis.

What about a/c use assumptions in the SSPs?

Without accounting for these feedbacks global mean temperature could be up to 0.3° C less, and we would be missing the significant changes to the energy system and regional changes. The community is moving toward more fully coupled simulations of the human earth system. This framework developed sets the stage for exploring feedbacks like, changes in water for energy, water for agriculture, [insert more feedbacks or give one detailed example(?)].

## 5 Acknowledgements

## References

- Li, D. H. W., Yang, L., & Lam, J. C. (2012). Impact of climate change on energy use in the built environment in different climate zones – A review. *Energy*, *42*(1), 103–112. <http://doi.org/10.1016/j.energy.2012.03.044>
- Isaac, M., & van Vuuren, D. P. (2009). Modeling global residential sector energy demand for heating and air conditioning in the context of climate change. *Energy Policy*, *37*(2), 507–521. <http://doi.org/https://doi.org/10.1016/j.enpol.2008.09.051>
- Auffhammer, M., & Mansur, E. T. (2014). Measuring climatic impacts on energy consumption: A review of the empirical literature. *Energy Economics*, *46*, 522–530. <http://doi.org/10.1016/j.eneco.2014.04.017>
- Yu, S., Eom, J., Zhou, Y., Evans, M., & Clarke, L. (2014). Scenarios of building energy demand for China with a detailed regional representation. *Energy*, *67*, 284–297. <http://doi.org/10.1016/j.energy.2013.12.072>
- Sharma, M., Chaturvedi, V., & Purohit, P. (2017). Long-term carbon dioxide and hydrofluorocarbon emissions from commercial space cooling and refrigeration in India: a detailed analysis within an integrated assessment modelling framework. *Climatic Change*, *143*(3-4), 503–517. <http://doi.org/10.1007/s10584-017-2002-4>
- Petri, Y., & Caldeira, K. (2015). Impacts of global warming on residential heating and cooling degree-days in the United States. *Scientific Reports*, *5*(1). <http://doi.org/10.1038/srep12427>
- Labriet, M., Joshi, S. R., Vielle, M., Holden, P. B., Edwards, N. R., Kanudia, A., ... Babonneau, F. (2013). Worldwide impacts of climate change on energy for heating and cooling. *Mitigation and Adaptation Strategies for Global Change*, *20*(7), 1111–1136. <http://doi.org/10.1007/s11027-013-9522-7>
- Calvin, K., Clarke, L., Edmonds, J., Eom, J., Hejazi, M., Kim, S., ... others. (2016). GCAM User Guide, version 4.3. Retrieved from <http://jgcri.github.io/gcam-doc/toc.html>
- M.A. Wise, K. V. C. (2011). *GCAM 3.0 Agriculture and Land Use: Technical Description of Modeling Approach*. PNNL-20971, Pacific Northwest National Laboratory, Richland, WA.
- Hartin, C. A., Patel, P., Schwarber, A., Link, R. P., & Bond-Lamberty, B. P. (2015). A simple object-oriented and open-source model for scientific and policy analyses of the global climate system–Hector v1. 0.

*Geoscientific Model Development*, 8(4), 939–955.

Eom, J., Clarke, L., Kim, S. H., Kyle, P., & Patel, P. (2012). China's building energy demand: Long-term implications from a detailed assessment. *Energy*, 46(1), 405–419.

Chaturvedi, V., Eom, J., Clarke, L. E., & Shukla, P. R. (2013). Long-Term Evolution of Building Energy Demand for India: Disaggregating End Use Energy Services in an Integrated Assessment Modeling Framework. Energy Modeling Forum, Stanford University.

Zhou, Y., Eom, J., & Clarke, L. (2013). The effect of global climate change, population distribution, and climate mitigation on building energy use in the US and China. *Climatic Change*, 119(3-4), 979–992.

Eom, J., Clarke, L. E., Kim, S. H., Kyle, G. P., & Patel, P. L. (2012). *China's Building Energy Use: A Long-Term Perspective based on a Detailed Assessment*. Office of Scientific and Technical Information (OSTI). Retrieved from <https://doi.org/10.2172/2F1034232>

Riahi, K., van Vuuren, D. P., Kriegler, E., Edmonds, J., O'Neill, B. C., Fujimori, S., ... Tavoni, M. (2017). The Shared Socioeconomic Pathways and their energy land use, and greenhouse gas emissions implications: An overview. *Global Environmental Change*, 42, 153–168. <http://doi.org/10.1016/j.gloenvcha.2016.05.009>

van Vuuren, D. P., Stehfest, E., Gernaat, D. E. H. J., Doelman, J. C., van den Berg, M., Harmsen, M., ... Tabeau, A. (2017). Energy land-use and greenhouse gas emissions trajectories under a green growth paradigm. *Global Environmental Change*, 42, 237–250. <http://doi.org/10.1016/j.gloenvcha.2016.05.008>

Fricko, O., Havlik, P., Rogelj, J., Klimont, Z., Gusti, M., Johnson, N., ... Riahi, K. (2017). The marker quantification of the Shared Socioeconomic Pathway 2: A middle-of-the-road scenario for the 21st century. *Global Environmental Change*, 42(Supplement C), 251–267. <http://doi.org/https://doi.org/10.1016/j.gloenvcha.2016.06.004>

Kriegler, E., Bauer, N., Popp, A., Humpenöder, F., Leimbach, M., Streffer, J., ... Edenhofer, O. (2017). Fossil-fueled development (SSP5): An energy and resource intensive scenario for the 21st century. *Global Environmental Change*, 42, 297–315. <http://doi.org/10.1016/j.gloenvcha.2016.05.015>

Zhou, Y., Eom, J., & Clarke, L. (2013). The effect of global climate change population distribution, and climate mitigation on building energy use in the U.S. and China. *Climatic Change*, 119(3-4), 979–992.

<http://doi.org/10.1007/s10584-013-0772-x>

(2007). M.L. Parry, O.F. Canziani, J.P. Palutikof, P.J. van der Linden and C.E. Hanson, Eds., Cambridge University Press, Cambridge, UK, 357-390.

Olonscheck, M., Holsten, A., & Kropp, J. P. (2011). Heating and cooling energy demand and related emissions of the German residential building stock under climate change. *Energy Policy*, 39(9), 4795–4806.

Zhou, J., Xue, Z., Du, Z., Melese, T., & Boyer, P. D. (1988). Relationship of tightly bound ADP and ATP to control and catalysis by chloroplast ATP synthase. *Biochemistry*, 27(14), 5129–5135. <http://doi.org/10.1021/bi00414a027>

Boyer, P. D. (1998). Energy Life, and ATP (Nobel Lecture). *Angewandte Chemie International Edition*, 37(17), 2296–2307. [http://doi.org/10.1002/\(sici\)1521-3773\(19980918\)37:17<2296::aid-anie2296>3.0.co;2-w](http://doi.org/10.1002/(sici)1521-3773(19980918)37:17<2296::aid-anie2296>3.0.co;2-w)

Zinszer, K., Morrison, K., Verma, A., & Brownstein, J. S. (2017). Spatial Determinants of Ebola Virus Disease Risk for the West African Epidemic.. *PLoS Curr*, 9.

Riahi, K., van Vuuren, D. P., Kriegler, E., Edmonds, J., O'Neill, B. C., Fujimori, S., . . . Tavoni, M. (2017). The Shared Socioeconomic Pathways and their energy, land use, and greenhouse gas emissions implications: An overview. *Global Environmental Change*, 42(Supplement C), 153–168. <http://doi.org/https://doi.org/10.1016/j.gloenvcha.2016.05.009>

Isaac, M., & van Vuuren, D. P. (2009). Modeling global residential sector energy demand for heating and air conditioning in the context of climate change. *Energy Policy*, 37(2), 507–521. <http://doi.org/10.1016/j.enpol.2008.09.051>

Wang, H., & Chen, Q. (2014). Impact of climate change heating and cooling energy use in buildings in the United States. *Energy and Buildings*, 82, 428–436. <http://doi.org/https://doi.org/10.1016/j.enbuild.2014.07.034>